AECL 11987

Reprinted from

journal of nuclear materials

Journal of Nuclear Materials 265 (1999) 161–177

Corrosion of stainless steel by gaseous I_2

J.C. Wren *, G.A. Glowa, J. Merritt

Fuel Safety Branch, Containment Chemistry Section, Atomic Energy of Canada Limited, Chalk River Laboratories, Chalk River, Ont., Canada K0J 1J0

Received 14 April 1998; accepted 14 August 1998

ELSEVIER

ELSEVIER

Journal of Nuclear Materials 265 (1999) 161–177

journal of nuclear materials

Corrosion of stainless steel by gaseous I_2

J.C. Wren *, G.A. Glowa, J. Merritt

Fuel Safety Branch, Containment Chemistry Section, Atomic Energy of Canada Limited, Chalk River Laboratories, Chalk River, Ont., Canada K0J 1J0

Received 14 April 1998; accepted 14 August 1998

Abstract

The adsorption and desorption of gaseous iodine on stainless steel was studied at low temperature under atmospheric conditions. Sorption kinetics were studied by measuring the ^{131}I tracer activity on a stainless steel coupon during loading and purging. Scanning electron microscopy (SEM) photographs and energy dispersive X-ray (EDX) analyses were also obtained at various stages of loading and purging. The iodine uptake and corrosion on stainless steel surface was extensive at room temperature, particularly in air. The adsorbed iodine desorbed only during purging with air and not with N_2. This desorption behaviour and the extensive iodine-catalysed corrosion in air are explained by the reaction of oxygen with FeI_2 to form iron oxyiodide (FeI_xO_y) solids, and by significant volume changes associated with the formation of FeI_2 and FeI_xO_y. These volume changes continuously generate cracks and grain boundaries through which I_2 can diffuse to react with Fe.

1. Introduction

Iodine is regarded as one of the most hazardous fission products that could be released from fuel in the event of a nuclear reactor accident. Under most accident conditions, the iodine released from fuel into the containment building would be primarily in its reduced state as cesium iodide, and thus would be easily dissolved in the water originating from the discharged coolant and any safety systems present [1–4]. However, in a fuel-handling accident in which fuel is assumed to be exposed to the dry oxidizing containment atmosphere during fuel heat-up, a large fraction of the iodine released from fuel may be in the form of gaseous I_2. Some Canadian Deuterium Uranium (CANDU® [1]) reactor safety analyses assume that, in this accident, iodine is released from fuel into containment entirely as I_2, but credit neither the iodine deposition on containment surfaces nor the removal of iodine by dousing water. This is not realistic or appropriate; not all iodine would escape the containment building because I_2, being a very reactive molecule, would be easily removed by natural processes (dissolution in water and deposition on various surfaces) or because of engineered processes (e.g., spray dousing), or because of both of these possibilities.

The work presented here was initiated to develop an understanding of the interaction of I_2 with a wide variety of reactor materials and surfaces that can be used to predict the iodine behaviour in containment following an accident. As stainless steel is one of the materials used in containment, the ability to predict the extent of I_2 interaction with steel surfaces following an accident is desirable. Although this work is most crucial to understanding the iodine behaviour in containment following a dry fuel handling accident in which the iodine is present mainly as I_2, it is also useful to other accident cases where, although the airborne iodine fraction is small, it is still present mainly as I_2. The results of this work may also be of interest to the Pressurised Water Reactor (PWR) safety analyses of other accidents. The current PWR safety analyses [5], subject to on-going debate [6], assume that the initial iodine speciation in containment following a Loss-of-Coolant Accident (LOCA) is I_2:CsI:organic iodide in the ratios 91:5:4.

Quantifying the interaction of iodine with stainless steel at ambient temperatures may also be important in

* Corresponding author. Tel.: +1-613 584 3311; fax: +1-613 584 1220; e-mail: wrenc@aecl.ca.

[1] CANDU® is a registered trademark of Atomic Energy of Canada Limited.

0022-3115/99/$ – see front matter
PII: S0022-3115(98)00504-2

any attempt to calibrate the gas sampling lines. Such lines are present in many nuclear power stations for various purposes. Depending upon the application, factors affecting the transmission of various species through these lines needs to be understood, and there is a potential for applying data on iodine sorption for that purpose.

Although iodine deposition on steel surfaces has been studied previously, most of these early studies were performed with the objective of quantifying iodine deposition in the primary heat transport system (PHTS) and, thus, dealt mostly with high temperatures (>200°C) in reducing H_2 and steam environments [7–32]. Low temperature data are scarce, and the results that do exist often appear to contradict those obtained in high-temperature studies. There is evidence that iodine chemistry at low temperatures is more complicated than at high temperatures [33,34]. We have studied, under ambient temperature and atmospheric conditions, iodine adsorption and desorption kinetics on various stainless steel surfaces (i.e., untreated, electropolished and nitric-acid treated), and performed the surface analyses at various stages of adsorption and desorption. Based on these results, potential mechanisms for the interaction of iodine with stainless steel are proposed.

2. Experimental

Iodine sorption behaviour on stainless steel surfaces was studied in the apparatus shown in Fig. 1. Coupons were placed in a glass flow cell and exposed to a continuous flow of N_2 or air containing I_2 at room temperature. No attempt was made to control relative humidity, but it was measured and found to be usually in the range of 32–35%. The iodine generation vessel contained 250 ml of a trace-labeled CsI solution. At the start of a test, the solution was acidified with 1 ml of dilute HCl and 5 ml of 0.1 M H_2O_2 was added to generate I_2. The pump then recirculated the gas flow through the iodine generator at 2 l/min, while a known fraction (about 5%) of the flow passed through a TEDA-impregnated charcoal filter. The ^{131}I activity accumulated on the filter was periodically measured to determine the gas phase iodine concentration. When the gas phase was approximately 1×10^{-9} mol dm^{-3} (ranging from 9×10^{-10} to 1.2×10^{-8} mol dm^{-3}), the coupon chamber was valved in to begin the adsorption onto the coupon. This concentration is of the order of the maximum I_2 concentration expected in a fuel handling accident, and also the gas phase iodine concentration observed in our intermediate scale studies in the Radioiodine Test Facility (RTF) under LOCA conditions (see Section 4 for more detail). Differences in iodine concentrations for each experiment are believed to be due to minor differences (such as pH, temperature) in each trace-labeled iodide solution. Loading was continued, in general, until saturation or a steady state in the adsorbed iodine concentration was reached.

The adsorbed iodine concentration was followed as a function of time during loading and purging through the use of a NaI gamma detector mounted next to the

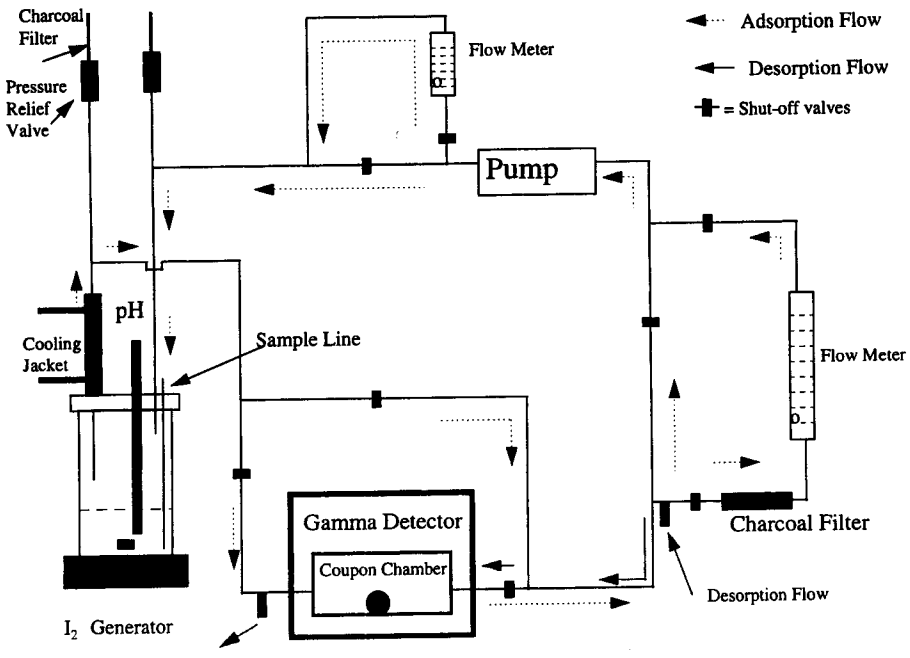

Fig. 1. Schematic diagram of iodine sorption apparatus.

coupon chamber. This counter was calibrated by appropriately scaling the data to an iodine loading obtained off-line in a well-type NaI detector. Data were corrected for background activity and ^{131}I decay before being converted to the adsorbed iodine concentration in units of mol cm^{-2}, and normalized to account for differences in the gas phase iodine loading concentration. Geometric coupon surface area was used to calculate the surface concentration, even though differences in surface roughness were evident in variously treated samples. The normalization with respect to the iodine loading concentration was based on the fact that both the iodine deposition velocity and saturation capacity have been observed to depend linearly on the iodine loading concentration [12,20].

Purging with N_2 or air followed once saturation was reached. The coupon chamber was then isolated and the appropriate desorption gas flow was so connected that it entered into the coupon chamber and exited through a carbon filter. The flow path during purging was somewhat different from loading and the gas flow rate during purging was half of the loading flow rate. The differences between the loading and purging flow conditions were mainly due to the convenience in setting up the test rig and should not affect the interpretation of the results. Desorption continued for at least 24 h, before the coupon was removed and placed in an inert atmosphere to await further analysis.

The stainless steel coupons (12.7 mm in diameter, 3 mm in thickness) were all prepared from 304-l stainless steel. Following a desired surface preparation, i.e. electropolished, nitric acid treated, or untreated, each coupon was washed, sequentially, in distilled water, 2-propanol, acetone and methanol. They were then dried at 70°C for 30 min and stored in a desiccator until required. During electropolishing, the coupon was placed in a polishing bath of H_3PO_4 (63%), H_2SO_4 (15%) and H_2O (22%). The coupon was then agitated in the bath for 30 min at approximately 5 V and 3 A. Nitric acid treatment consisted of placing the coupon in concentrated nitric acid for 2 h.

Iodine loading and purging on the samples for surface analyses were prepared in much the same manner, except the iodine source was not trace labeled. Samples were removed from the coupon chamber and stored in a vial until the surface analysis could be performed. Although the samples were stored under nitrogen between analysis and loading, rigorous attempts to exclude oxygen were not made. Moreover, even the nitrogen used during loading and purging is suspected to have contained trace amounts of oxygen.

Photographs obtained from secondary electron images using a JOEL JSM-6300V scanning electron microscope (SEM) and the energy dispersive X-ray (EDX) spectra acquired on the same system were the main surface analyses used in this study. The EDX spectroscopy provides qualitative elemental analysis. The X-ray photoelectron spectroscopy (XPS) analysis was also performed on a few samples to determine the nature of iodine adsorbed on stainless steel surface.

3. Results

3.1. Kinetics of I_2 interaction with stainless steel

3.1.1. Iodine sorption behaviour during loading

Figs. 2–6 show the adsorbed iodine concentration as a function of time observed during loading and during purging on untreated, electropolished and nitric-acid treated coupons. On all three stainless steel surfaces, the adsorbed iodine concentration initially increases linearly with time but then slows down. A steady state was reached after ~10 h in all cases, except for the loading of

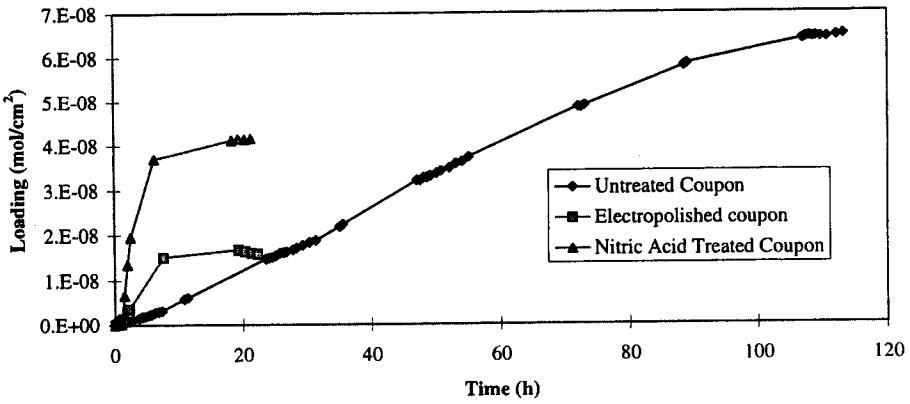

Fig. 2. Concentration of adsorbed iodine on various stainless steel coupons during loading in N_2. Gas-phase iodine concentrations were untreated, 8.7×10^{-13} mol cm^{-3}; electropolished, 3.5×10^{-12} mol cm^{-3}; and nitric acid, 5.7×10^{-12} mol cm^{-3}.

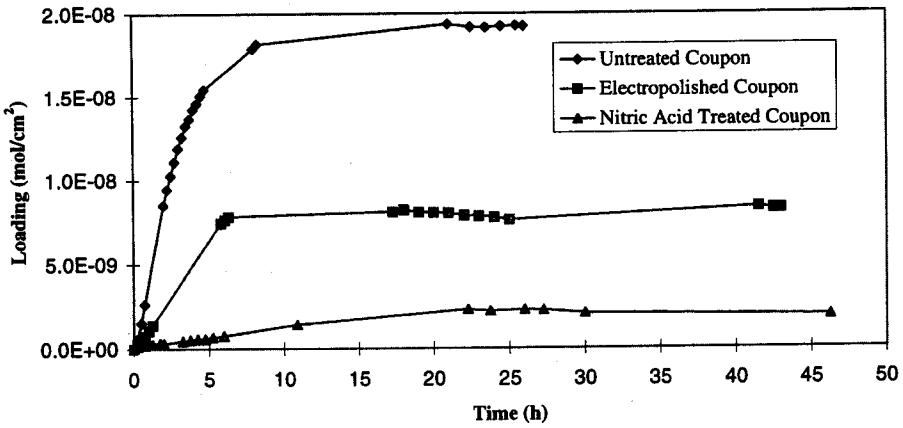

Fig. 3. Concentration of adsorbed iodine on various stainless steel coupons during loading in air. Gas-phase iodine concentrations were untreated, 2.2×10^{-12} mol cm^{-3}; electropolished, 2.3×10^{-12} mol cm^{-3}; and nitric acid, 1.3×10^{-12} mol cm^{-3}.

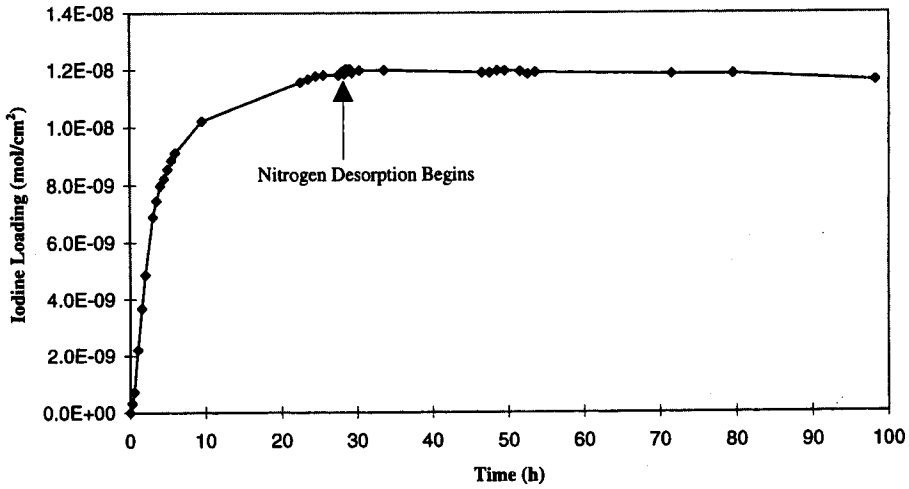

Fig. 4. Iodine on untreated coupon during loading in air and subsequent purging in N_2. The gas phase iodine concentration during loading was 2.1×10^{-12} mol cm^{-3}.

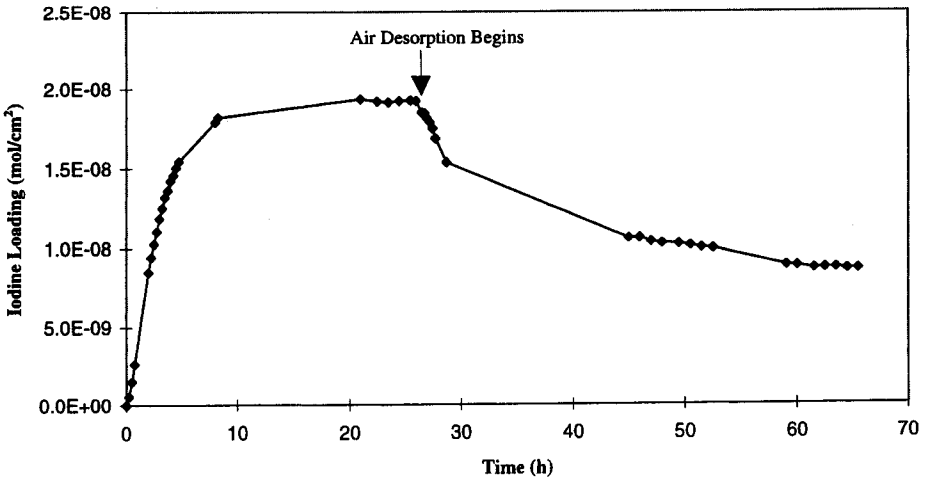

Fig. 5. Iodine on an untreated coupon during loading and purging in air. The gas phase iodine concentration during loading was 2.2×10^{-12} mol cm^{-3}.

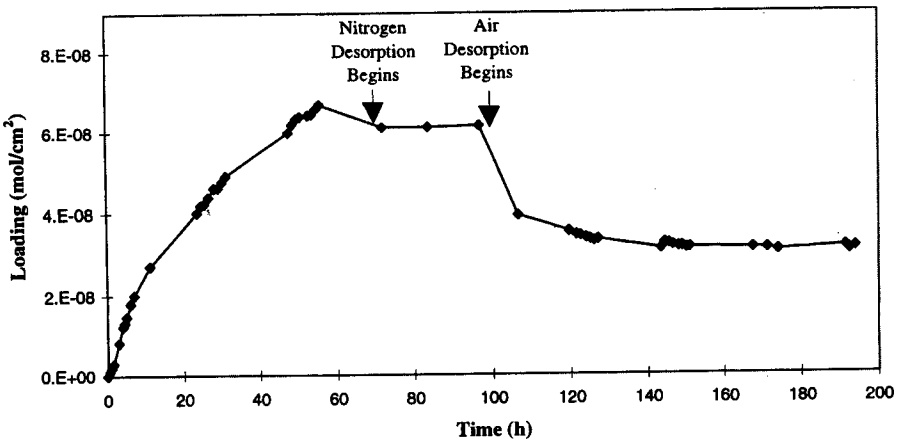

Fig. 6. Iodine loading in N_2 followed by purging with N_2 and then with air. The gas phase iodine concentration during loading was 4.1×10^{-12} mol cm^{-3}.

an untreated surface in N_2. In the latter case, the adsorbed iodine concentration increased linearly for a long (>100 h) time (Fig. 2).

Two adsorption parameters were extracted from the adsorption curve: the apparent iodine deposition velocity from the initial slope and the saturation capacity from the final steady-state concentration. These parameter values are listed in Table 1.

The saturation capacity was observed to increase linearly with I_2 loading concentration and is listed in Table 1 in units of cm, i.e., normalized to the iodine loading concentration. The iodine deposition rate also showed a linear dependence on the I_2 loading concentration and is tabulated (Table 1) as an apparent deposition velocity, v_{app}. The deposition velocity is essentially the rate coefficient of the overall adsorption process represented by

$$I_2(g) \rightarrow 2I(ad), \tag{1}$$

with an overall rate law

$$d[I(ad)]/dt = v_{app}[I_2(g)]. \tag{2}$$

Assuming a constant $[I_2(g)]$,

$$[I(ad)]_t = v_{app}[I_2(g)]_0 t. \tag{3}$$

It should be noted that the use of the apparent deposition velocity does not necessarily suggest that the adsorption of iodine on a steel surface can be described simply by Reaction (1). The detailed sorption mechanism needs to be elucidated.

When loading was performed in a near-oxygen-free (i.e., humid N_2/I_2) atmosphere, the apparent iodine deposition velocity on all three surfaces was observed to be about the same. However, the saturation capacity was about an order of magnitude greater on an untreated surface than on an electropolished or nitric-acid treated surface. Although the microscopic surface areas of the coupons were not determined in these studies, SEM images showed that electropolishing and acid-treatment smoothed the surfaces, reducing the effective surface areas (see Section 3.2) of the treated coupons.

In humid air/I_2, the apparent deposition velocity was greatest on an untreated surface, followed by an electropolished surface and then nitric-acid treated stainless steel surface (Fig. 3). The saturation capacity showed the same trend.

For an untreated surface, the presence of oxygen in the carrier gas appears to increase the apparent deposition velocity but lower the iodine adsorption capacity. For an electropolished surface, there appeared to be no significant changes in the iodine deposition velocity and saturation capacity because of the presence of oxygen in the gas flow mixture. For a nitric-acid treated surface, both the apparent deposition velocity and the saturation capacity were reduced in humid air/I_2, compared with that observed in humid N_2/I_2.

Table 1
Adsorption parameters observed for I_2 on stainless steel surfaces

Type of surface	Deposition velocity (cm h^{-1})		Normalized saturation capacity (cm)	
	In air	In N_2	In air	In N_2
Untreated	$2.0 \pm 0.5 \times 10^3$	$7 \pm 2 \times 10^2$	$2.0 \pm 0.5 \times 10^4$	$>8 \pm 2 \times 10^4$
Electropolished	$5 \pm 2 \times 10^2$	$6 \pm 2 \times 10^2$	$4 \pm 2 \times 10^3$	$5 \pm 2 \times 10^3$
Nitric acid treated	$1 \pm 0.5 \times 10^2$	$10 \pm 3 \times 10^2$	$2.0 \pm 0.5 \times 10^3$	$8 \pm 2 \times 10^3$

3.1.2. Desorption of iodine during purging

The reaction of oxygen with adsorbed iodine appears to be mainly responsible for the desorption of iodine from stainless steel surfaces at room temperature. Desorption of iodine from all stainless steel surfaces was negligible during purging with N_2 (Fig. 4). Significant desorption was observed only during purging with air (Fig. 5). This was particularly apparent when the purging gas was switched from N_2 to air (Fig. 6).

The desorption of iodine during purging with air did not follow simple first-order kinetics. Complete desorption of iodine was not obtained in any case, indicating that some iodine was irreversibly adsorbed. When this fraction was accounted for, the remainder of the iodine showed first-order desorption kinetics (see Section 4 for a detailed discussion).

3.1.3. Multiple cycle studies

We also performed multiple cycles (up to four) of loading and purging. The normalized adsorption curves during iodine loading in air on an untreated surface were very similar (Fig. 7(a)), although the absolute adsorbed concentration varied from cycle to cycle depending mainly on the gas-phase I_2 concentration. The adsorbed iodine concentration in the first cycle shows a slower increase for a short period, probably because of initial adsorption on defect sites. This initial rate is thought to vary considerably from one surface to another. However, after the initial delay, the adsorbed iodine concentration increased at a rate similar to those observed in subsequent cycles. In contrast, the desorption during purging with air progressively slowed down, and the fraction of iodine released was smaller with each cycle (Fig. 7(b)). The other surface preparations showed similar behaviour.

3.2. Surface analysis

3.2.1. Prior to iodine exposure

Analyses using SEM and EDX were performed on the surfaces at various stages of the iodine sorption. The SEM photographs of these surfaces taken prior to

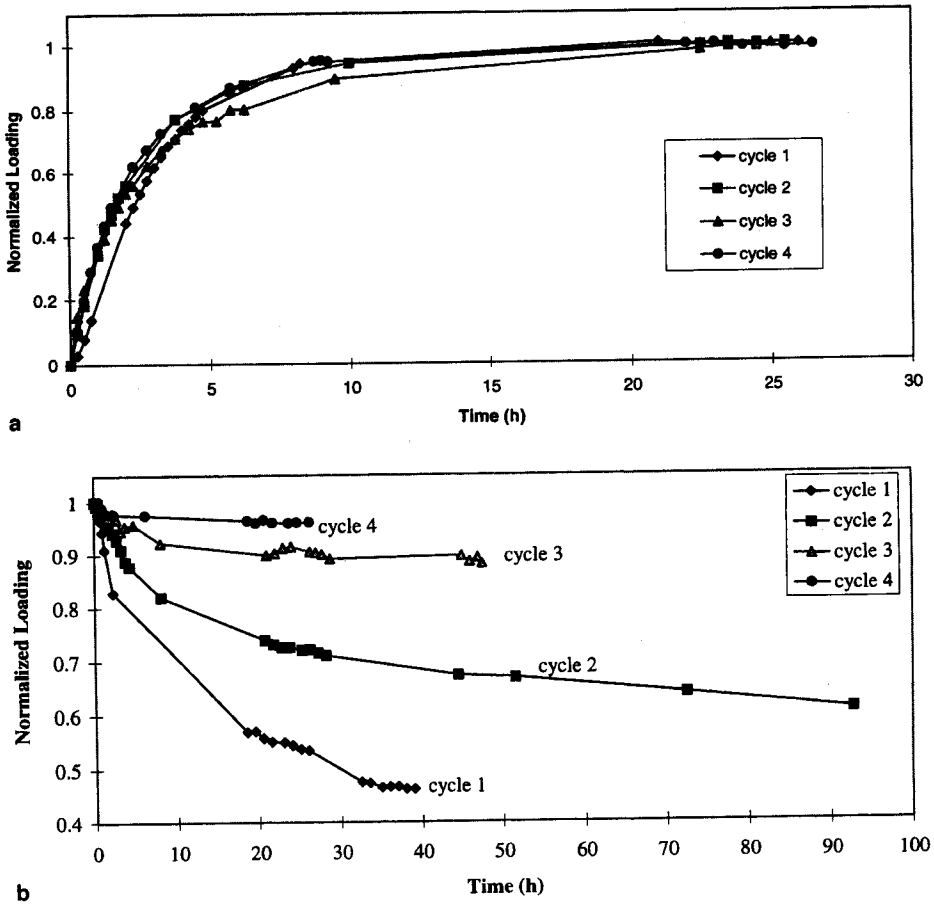

Fig. 7. (a) Iodine loading of four consecutive cycles on an untreated surface normalized to the maximum concentration adsorbed. (b) Normalized Iodine loading during the desorption phase of four consecutive adsorption/desorption cycles using the same untreated coupon.

exposure to I_2 show that electropolishing and nitric acid treatments smooth the stainless steel surface, reducing the effective surface area (Fig. 8(a)). It was speculated that these surface treatments might enhance chromium content on the surface; however, this could not be observed in EDX spectra. The EDX of treated and untreated surfaces show the same ratio of the Fe (at 6.4 keV) to Cr peak (at 5.4 keV). The oxygen peak is not prominent in the EDX spectra, probably because the oxide layers are thin on the stainless steel coupons. A typical EDX spectrum of a surface prior to I_2 exposure is given in Fig. 8(b).

3.2.2. Untreated coupons exposed to $I_2(g)$

3.2.2.1. Loading in N_2. Figs. 9–11 show the SEM and EDX of untreated stainless steel following exposure to an air or N_2 stream containing I_2. Following loading in N_2, the surface appears to become smoother, which may indicate that the iodine adsorption is rather uniform. The surface was also dotted with particles of the order of 0.1 μm (Fig. 9(a)). No further change was observed as a result of subsequent purging with N_2. These particles appear to be spread evenly over the surface, but are somewhat more concentrated around defected areas of the surface. The EDX spectrum suggests that these particles are iodine compounds (Fig. 9(b)). The particles also contained higher amounts of sulfur and copper than the bulk surface.

We have performed XPS analysis on iodine deposits that show iodine peaks at −630.9 and −619.5 eV, suggesting that iodine is in the form of metal iodides. It is difficult, however, to distinguish between specific metal iodides (iron, chromium or nickel iodides) because of the similarities in their binding energies [35].

Bigger iodide containing particles of ~10 μm, which were sometimes observed in a few places, appeared to be due to contamination during the preparation of the coupons, i.e. cutting and polishing, as shown by the tungsten (W) and silicon (Si) peaks in their EDX spectra. This suggests that the contaminated areas facilitated iodide scale formation.

3.2.2.2. Loading in Air. . The change on an untreated surface following I_2 loading in air was significant with the formation of large solid particles ~1 μm in depth and ~10 μm in width (Fig. 10(a) and 11). These solids appear to have grown up to ~100 μm in length along the direction of the surface grain, but show cracks about every ~10 μm probably because of significant volume changes as a result of the growth of the solid.

The EDX of this type of solid shows iodine peaks at ~4 keV and an oxygen peak at ~0.5 keV (Fig. 10(b)). The EDX also shows an increased ratio of Fe to Cr compared to the areas unaffected by iodine or the controlled samples. The EDX spectrum of the unaffected areas shown in Fig. 10(a) was observed to be the same as that of the samples before adsorption, as shown in Fig. 8(b). All the solids formed on any surface in this study showed an increased ratio of Fe to Cr in their EDX spectra, compared to an unaffected area. (It should be noted that the peak intensity of EDX is difficult to correlate to concentration due to different X-ray dispersion on different surfaces. However, since these solids are large and have relatively smooth surfaces and the X-ray energies of Cr and Fe are similar, qualitative comparison of the EDX peaks from these solids and from unaffected areas may still be made. Furthermore, because the solids are porous and only about 1 μm thick, the areas underneath the solids may also have contributed to the EDX signal.) The increase in the Fe to Cr ratio and the presence of oxygen indicate that a significant amount of iron had reacted and then migrated to the surface to form FeI_2, FeIO and Fe_xO_y. These solids had also grown outward, further supporting the migration of Fe to the surfaces (further discussion in Section 4).

The SEM of the stainless steel surfaces exposed to I_2 in air also show areas where it appears that large sections of solid scale had grown but had fallen off, exposing the metal surface underneath (Fig. 10(a)). (The fraction of these exposed areas compared to those covered with solids was small.) The areas where the sections of solid scale had fallen off appear to be resistant to further iodine adsorption. The exact locations of some spots for SEM measurement were marked and revisited. We did not observe any further solid formation on these areas when the surface was exposed to another cycle of loading and purging. We postulate that this is due to the richer Cr content of these areas which results from the migration of Fe to the surface for the reactions with I_2 and O_2. The chromium enriched surface can form more stable and subsequently unreactive chromium oxide layers during the exposure to air.

No further change in the SEM images or EDX spectra was observed as the result of subsequent purging with N_2. However, it appeared that during air purging after iodine loading in air, the cracks widened and the solids formed during loading were attacked (compare Fig. 11 with Fig. 10(a)). One possibility is that iron-iodide-oxides were continually formed from FeI_2 during purging in air, progressively shrinking the solids and widening the cracks.

3.2.3. Nitric acid treated coupons exposed to $I_2(g)$

The effect of the nitric acid treatment is to smooth the surface, by dissolution of surface asperities. Irregularities in the metal surface are removed under passive conditions by a variable dissolution rate mechanism. Nitric acid treatment is commonly used to passivate steel surfaces.

After one cycle of loading and purging in air, large rounded deposits are left in a circular pattern, which

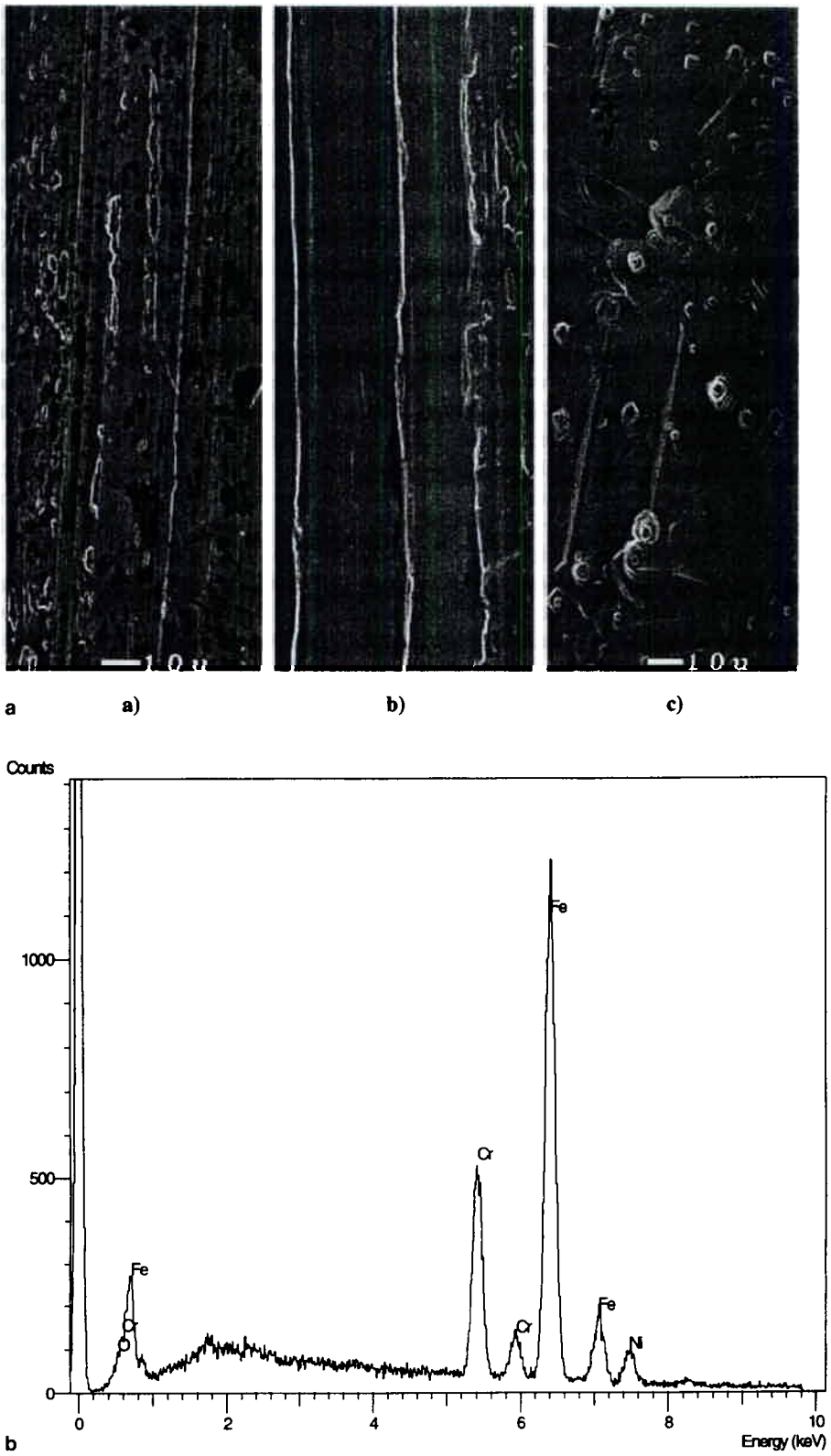

Fig. 8. (a) SEM photograph of surface of (a) untreated, (b) nitric acid treated, and (c) electropolished coupon prior to iodine adsorption. (b) Typical EDX spectrum of coupon surface prior to iodine adsorption.

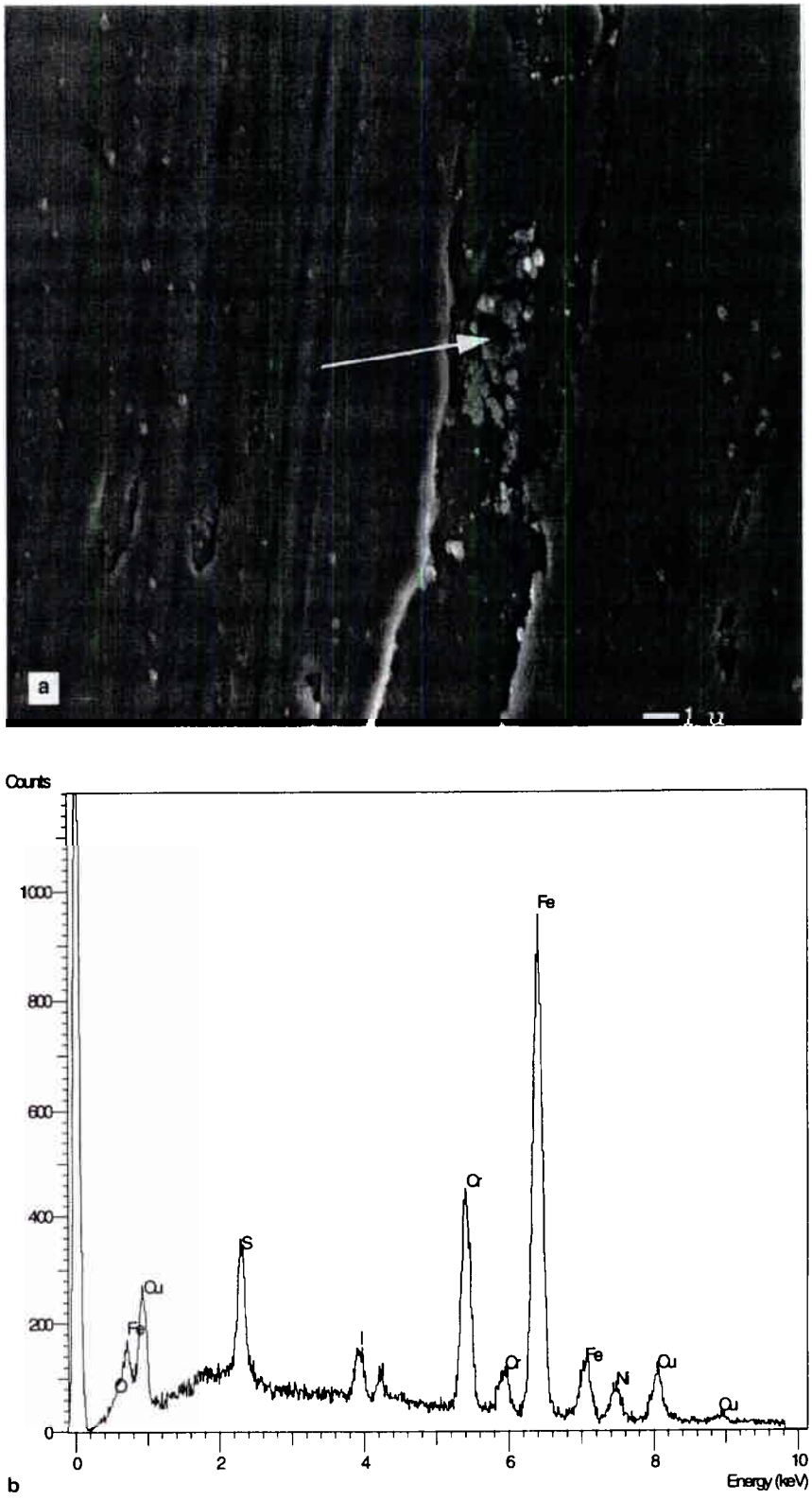

Fig. 9. (a) SEM Photograph of untreated coupon after one cycle of iodine adsorption and desorption in nitrogen. Arrow shows approximate location of EDX analyses. (b) EDX spectrum of area indicated in Fig. 9(a).

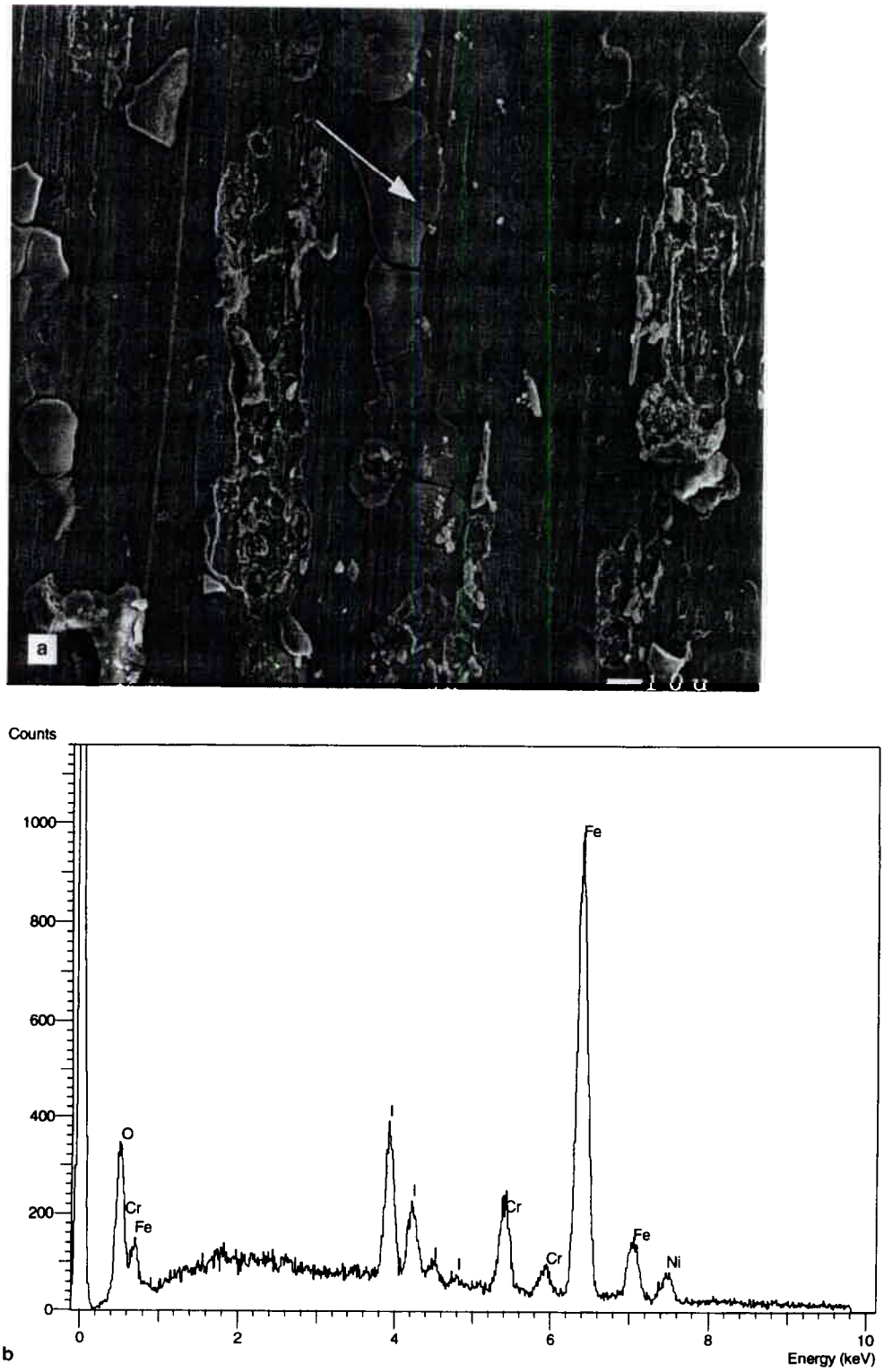

Fig. 10. (a) SEM photograph of surface of an untreated coupon after air adsorption and N_2 desorption. White arrow indicates approximate location where EDX analysis was made. (b) EDX spectrum of area indicated in SEM photograph in Fig. 10(a).

seems to follow the remnants of grooves cut into the surface during production of the coupon (Fig. 12(a)). This suggests that iodine-assisted corrosion occurs more readily at the faults in the surface structure.

Fig. 11. SEM photograph of surface of untreated coupon after iodine adsorption in air and desorption in air.

which are less plentiful than on the untreated coupons.

The growth structures seem to be a mixture of metal iodides and oxides, much like those seen on the untreated surfaces. The deposits seem to be larger (~50 μm across), but fewer, which may be due to the decrease in the number of sites that can initiate metal iodide growth. The acid treatment may also have decreased the amount of Fe available for iodine reaction, making iodide (and oxide) formation less favourable but more orderly. Some of the deposits are cracked, which may be due to a volume change as iodine is replaced by oxygen in the solid matrix.

3.2.4. Electropolished coupons exposed to $I_2(g)$

Electropolishing is a process of smoothing a metal surface to produce a bright surface through anodic dissolution in an acidic (or basic) solution (Fig. 8(a)). Material is removed from the surface in such a manner that peaks, depressions and cracks are smoothed out, leaving a less defective, cleaner surface without the problems associated with a mechanical preparation. Mechanical processes (cutting and polishing) tend to leave stressed and disturbed regions of surface metal which may have properties (electrochemical, mechanical, reflective) that differ from those of the bulk metal.

Prior to adsorption, the electropolished coupon surface displays pitting, possibly because of the dissolution of non-metallic inclusions, but shows less of the original coupon cut marks. Most of the iodine deposition on the electropolished surface seems to have been initiated in the pits that were formed during electropolishing. The deposits are similar in size to the original pits, and the solid seems to be growing inward (Fig. 13). The EDX spectrum of the material in the pits shows iodine peaks.

4. Discussion

Stainless steel is a complex alloy, composed principally of iron, nickel and chromium, but also contains numerous lesser alloying and trace elements. Moreover, the metal surface is normally rough and covered by oxides whose thickness and composition may vary substantially. As a result, a stainless steel surface offers a wide variety of adsorption or reaction sites that have different affinities for iodine. The availability of reactive species, metallic elements or their cations or film-forming anions, will also be very complex and may be important in determining the kinetics of the stainless steel interaction with iodine. Surface treatments, such as preoxidation, electropolishing and mechanical polishing, prior to exposure to iodine, will change the surface morphology, area and composition (including the oxide). Because halogens are known to cause corrosion of stainless steel surfaces, iodine-catalysed corrosion may be an important factor under humid conditions [9,10].

4.1. Nature of adsorbed iodine

It has been speculated that iodine is mainly physically adsorbed on stainless steel surfaces at room temperature. However, desorption of iodine from iodine-loaded stainless steel surfaces was observed only during purging with air but not with N_2, indicating that the iodine deposited on stainless steel at this temperature is not physically adsorbed but chemically bound on the surfaces.

The XPS analysis of the iodine deposited on stainless steel showed that it is in the −1 oxidation state as metal iodide (the results not shown here). Rosenberg et al. [12] studied the dissolution of iodine from iodine-saturated stainless steel surfaces into I_2, FeI_2 and other iodide saturated water and established that iodine is adsorbed mainly as FeI_2. In their study, iodine was loaded on stainless steel at 115°C. We expect that iodine also adsorbs initially on defect sites to form solid FeI_2 at room temperature. Further iodination to form FeI_3 is not likely since it is thermodynamically less stable than FeI_2. The oxides of iron in an oxidation state greater than +2 are also more thermodynamically stable in air than FeI_2. Thus the reaction of Fe^{2+} and I_2 can be ruled out, and FeI_2 must be formed from iron in an oxidation state less than +2 (referred to as elemental Fe hereafter). In air, the adsorbed iodine appears to react further with oxygen, forming FeI_xO_y. The exact nature of the solids formed was not determined in this study, but is thought to consist of FeI_2, FeIO and iron oxides (for further discussion see below).

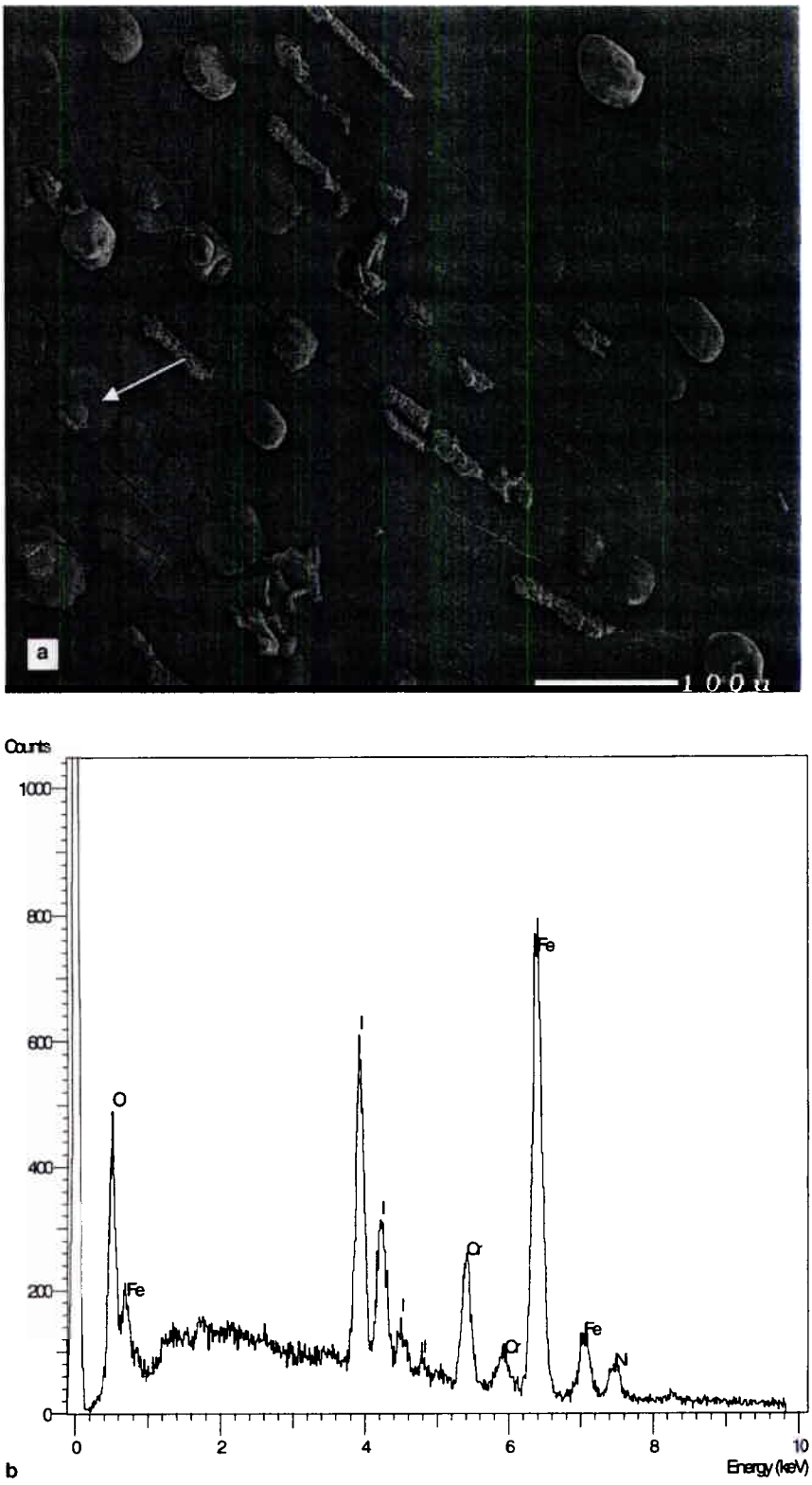

Fig. 12. (a) SEM photograph of surface of nitric acid treated coupon after first cycle. (b) EDX spectrum from area indicated in Fig. 12(a).

It has been speculated that, under humid conditions, the iron iodide forms a stable hydrate, $FeI_2 \cdot 4H_2O$ [12]. The thermodynamic properties of this species are not known. From comparison with analogous chloride

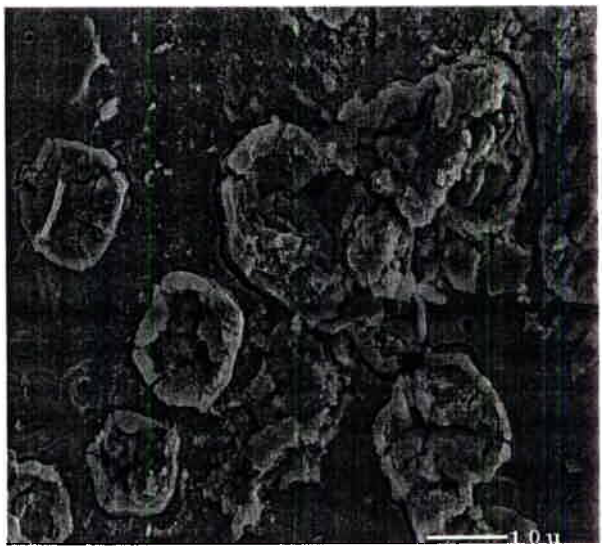

Fig. 13. SEM photograph of surface of electropolished coupon after iodine loading and desorption.

compounds [36], we speculate that $FeI_2 \cdot 4H_2O$ is as stable as most iron oxides and that further reaction with oxygen is not favourable. If hydrated iron iodide is the main species formed during iodine adsorption, then the desorption during air purging following loading in N_2 should be different from that following loading in air. Their first-order desorption rate constants were very similar, suggesting that formation of $FeI_2 \cdot 4H_2O$ is not important under our experimental conditions.

Nickel is also known to adsorb iodine, but the adsorption capacity of bulk metal Ni for I_2 was observed to be much smaller than that of Fe [12]. The reactivity of the nickel in stainless steel with iodine is not known. Chromium enrichment in stainless steel is known to increase its resistance to further oxidation by forming a protective oxide layer. The protective chromium-based oxide films may also be less reactive toward I_2.

4.2. Iodine interaction with untreated stainless steel in N_2

On untreated stainless steel, considerably different iodine sorption behaviour and surface changes were observed, depending on whether the iodine loading was done in N_2 or air. After loading in N_2, the surface appeared to be smoother on the SEM picture, indicating that a relatively uniform FeI_2 layer was formed on the surface. However, this film could not be confirmed by EDX because of the large contribution from the metal underneath the thin FeI_2 layer to the spectra. The EDX of the area containing the sub-micrometre particles shows that the particles are iodine compounds, presumably FeI_2.

The amount of iodine adsorbed on the untreated stainless steel after ~50 h loading in N_2 was about 1×10^{-7} mol cm^{-2}. Assuming randomly oriented FeI_2 'molecules' on the geometric surface area (~21 $Å^2$ FeI_2 area [37]), the amount of iodine adsorbed during the first cycle corresponds to ~126 monolayers (a depth of 58 nm). Because a steady state in the adsorption curve was not achieved within the 50 h loading period, the adsorbed amount is far less than the maximum adsorption capacity of the untreated surface for I_2 in N_2.

The reaction of iodine with an untreated stainless steel surface in N_2 is extensive. Such extensive reaction with I_2 without the need for the presence of a liquid electrolyte at room temperature is somewhat perplexing. The migration of elemental Fe through the FeI_2 solid should be negligible at room temperature. Because of this, iodine sorption through tiny droplets or a thin film of water (formed on the surface under humid conditions) has been proposed [38]. However, the iodine adsorption behaviour and the resulting surface changes were very different in N_2 and air atmospheres in this study, while the relative humidity was the same. This suggests that a moisture-mediated reaction is not the primary mechanism.

The adsorbed iodine concentration on an untreated surface during loading in N_2 shows a linear increase for a long time, following an initial rapid transient (Fig. 6). The rapid initial adsorption is probably the result of the iodine reaction at defect sites readily available on an untreated surface. This initial adsorption rate is thus expected to vary considerably from one surface to another. In fact, in the other case of N_2 loading (Fig. 2), the initial rate was slower and lasted for a shorter time. The later linear increase showing a constant adsorption rate observed for a long time without reaching a steady state is rather uncommon. One potential explanation for the extent of the gas/solid iodine reaction with stainless steel in N_2 is that the volume change caused by the formation of FeI_2 scale creates grain boundaries and cracks through which I_2 can diffuse to react with elemental Fe underneath the scale. With the formation of cracks accompanying film growth, the reaction of gas molecules with elemental metal can continue for a long time at a constant reaction rate.

4.3. Iodine interaction with untreated stainless steel in air

The adsorption capacity of an untreated stainless steel surface for I_2 was smaller for iodine loading in air than in N_2. However, the corrosion appears to be much more extensive in air, and the resulting surface was covered with large deposits about 20 μm in width and about 1 μm in depth. The EDX spectra of these solids show a large oxygen peak and an increased Fe to Cr peak ratio, suggesting extensive preferential migration of Fe and the formation of Fe–I–O compounds. Iodine was released during purging with air in all cases, but complete desorption of iodine was not obtained in any case.

We postulate that the following reactions occur in the presence of air:

$$Fe + I_2 \rightarrow FeI_2, \tag{4}$$

$$FeI_2 + \frac{y}{2}O_2 \rightarrow FeI_xO_y + \left(1 - \frac{x}{2}\right)I_2, \tag{5}$$

where FeI_xO_y represents a mixture of iron iodides and iron oxides. Some of this mixture is evidently capable of further reaction with oxygen to liberate iodine, but some iodine is bound either in particularly stable compounds or in film regions relatively inaccessible to atmospheric oxygen.

It appears that iodine adsorbs more easily on the FeI_xO_y mixture than on an untreated surface: the initial iodine adsorption rate was greater in the presence of oxygen than in N_2, and further growth is fastest on the initial reaction sites resulting in larger scale-particle formation. The different film growth behaviour observed in air compared to that in N_2 is considered to be the result of the oxygen reaction. The scale formation in air is discussed later.

We have analyzed the iodine desorption in more detail. We assume that iodine exists in two forms, FeI_2 and FeI_xO_y and that all the iodine in the oxy-iodide is 'trapped'. During purging oxidation, a fraction of iodine as FeI_2 is released (fraction $=f$) and the remainder $(1-f)$ forms FeI_xO_y. With these assumptions, the rate laws for adsorbed iodine during air purging become

$$\frac{d[FeI_2]}{dt} = -k_d[O_2][FeI_2], \tag{6}$$

$$\frac{d[I_r]}{dt} = (1-f)k_d[O_2][FeI_2], \tag{7}$$

where $[I_r]$ represents the adsorbed concentration of iodine that becomes trapped in the matrix of FeI_xO_y, k_d is the rate constant of the oxygen reaction. The solutions to the differential equations are

$$[FeI_2]_t = [FeI_2]_0 \exp(-k_d[O_2]t), \tag{8}$$

$$[I_r]_t = [I_r]_0 + (1-f)[FeI_2]_0(1 - \exp(-k_d[O_2]t)), \tag{9}$$

where $[FeI_2]_0$ and $[I_r]_0$ are the concentrations of FeI_2 and I_r at the start of purging.

The total adsorbed iodine concentration is then

$$[totalI]_t = [FeI_2]_t + [I_r]_t \tag{10}$$

or

$$[totalI]_t = [I_r]_0 + (1-f)[FeI_2]_0 + f[FeI_2]_0 \exp(-k_d[O_2]t). \tag{11}$$

This simple model fits the iodine desorption behaviour observed in this study, with the final adsorbed iodine concentration approaching

$$[totalI]_f = [I_r]_0 + (1-f)[FeI_2]_0. \tag{12}$$

Eq. (11) can be rearranged to give

$$\ln([totalI]_t - [totalI]_f) = \ln\left(f[FeI_2]_0\right) - k_d[O_2]t. \tag{13}$$

The iodine desorption curves observed in the multiple cycle study in air (Fig. 7(b)) are re-plotted in Fig. 14, showing the fit to Eq. (13). All the desorption data during air purging give the same rate constant:

$$k_d[O_2] = 0.09 \pm 0.03\ h^{-1} \tag{14}$$

regardless of the surface preparation (i.e., untreated, electropolished or nitric acid), iodine loading atmosphere (i.e. in N_2 or air) or number of cycles. This suggests that the rate-determining step for the iodine desorption in air is the oxidation of the originally formed iodide and not a mass transport process.

The fraction of adsorbed iodine that is removed during purging, however, decreased progressively with increasing number of loading and purging cycles, as seen in Fig. 7(b). The increase in the fraction, $1-f$, as the cycle progresses or as the corrosion of the surface progresses, indicates that, as FeI_xO_y solid builds up, iodine becomes easier to trap in the matrix.

Unlike the case of the iodine loading in N_2, iodine adsorption in air reached an adsorption limit. However, the amount of iodine adsorbed then increased in the subsequent cycle of purging and loading (Fig. 7(a)). This suggests that the iodine adsorption limit was reached because the steady-state iodine desorption rate becomes equal to the adsorption rate, resulting in zero additional net adsorption. Purging somehow provides access to fresh Fe metal (perhaps through film morphology changes and cracking) allowing for the additional net adsorption in each cycle. However, as the number of loading and purging cycles increases, or as the corrosion progresses, the fraction of iodine desorbed by the oxygen reaction becomes smaller (Fig. 7(b)). By the time the fourth cycle of loading and purging was performed, iodine desorption was negligible, yet the iodine adsorption reached a steady state. This suggests that the iodine adsorption rate also slows down as the corrosion progresses to limit the iodine adsorption.

As mentioned earlier, iodine seems to adsorb more easily on the FeI_xO_y mixture than on an untreated surface, evidenced by observations that the initial iodine adsorption rate was greater in the presence of oxygen than in N_2 and that further growth is fastest on the initial reaction sites resulting in larger scale-particle formation. The different film growth behaviour observed in air compared with that in N_2 is considered to be the result of the oxygen reaction. The rate of Reaction (5) appears to be of a similar order to that of Reaction (4), and the formation of FeI_xO_y and the accompanying surface morphology changes are thought to control the iodine adsorption behaviour.

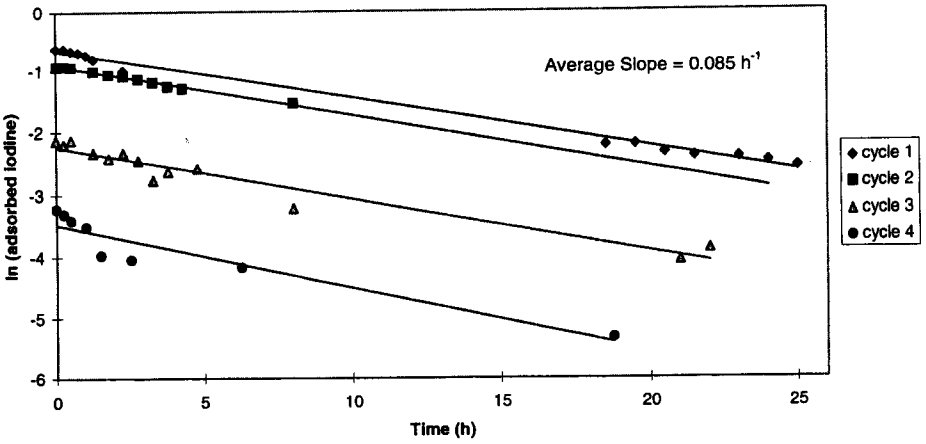

Fig. 14. Log plot of the loading in four consecutive cycles, fitted to Eq. (13).

We postulate the following processes (shown schematically in Fig. 15) to account for the observed iodine interaction with stainless steel in air. Reactions (4) and (5) are responsible for the scale formation. The scale formed by the fast reactions has many defect sites, thus acting as a semi-conductor which facilitates the migration of Fe, I_2 and O_2. The mechanism of forming a semi-conductor scale due to fast oxidation has been proposed for the oxidation of stainless steel at high temperatures [39]. Although our studies were performed at low temperature, the addition of I_2 enhances the corrosion rate to the point where a similar semi-conductor scale may be formed, allowing Reactions (4) and (5) continue extensively. Furthermore, the volume changes that are due to the formation of FeI_xO_y scale create cracks that further facilitates I_2 transport to react with elemental Fe underneath the scale to form FeI_2, and O_2 transport through the cracks to react with FeI_2. During purging, O_2 continuously migrates to the FeI_2 and reacts. More defect sites are created in the scale and the cracks widen at a faster rate during purging without Reaction (4). As the FeI_xO_y layer thickness increases with increasing number of loading and purging cycles, it becomes increasingly difficult for I_2 and O_2 to diffuse through the scale (probably as a result of Fe depletion), resulting in an increase in the fraction $(1 - f)$ with increasing number of cycles. The proposed mechanism may be one of the simplest explanations and is by no means complete. Future adsorption experiments are planned, including cross-sectional analysis of specimens, which will help pin-point the mechanism for the iodine interaction with stainless steel.

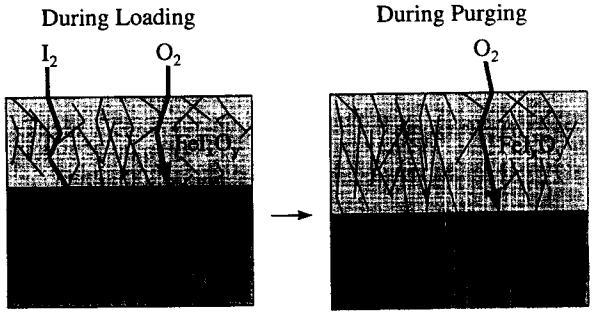

Fig. 15. Iodine interaction with stainless steel in air.

As mentioned in Section 2, the maximum iodine concentration expected in a fuel handling accident is expected to be less than 1×10^{-9} mol dm^{-3}. If one fuel bundle is assumed to be completely oxidized and the total iodine inventory of the bundle is released as I_2 all at once in a fuel handling accident, the iodine concentration in the atmosphere of the containment building would be 10^{-10}–10^{-9} mol dm^{-3}. The concentration is also comparable to typical gas phase iodine concentrations that are observed in the RTF under LOCA conditions. With an initial iodine concentration in the aqueous phase of 1×10^{-5} mol dm^{-3}, the gas phase iodine concentrations in the RTF range from about 1×10^{-8} to 1×10^{-12} mol dm^{-3} depending upon parameters such as radiation and pH [40–42]. Although it should be verified, we believe that this model should be valid for concentrations less than 1×10^{-9} mol dm^{-3}. However, the mechanism may change at much higher concentrations due to a quicker buildup of hygroscopic FeI_2 attracting moisture, which would alter the FeI_2 into hydrated compounds, making desorption less favorable. The presence of water droplets could then change the mechanism entirely.

4.4. Iodine interaction with pre-treated stainless steel

For electropolished surfaces, the addition of oxygen did not appear to make much difference to the iodine deposition rate or the adsorption capacity. The protective oxide layer formed during electropolishing is more defect-free than that on an untreated surface. During the

time scale of our experiments, iodine is deposited mainly in a limited number of pits. The growth of smaller scale particles may prevent the morphology changes that influence the corrosion of the untreated surfaces.

On nitric-acid treated stainless steel, the presence of air lowered the deposition rate and the adsorption capacity. The simplest explanation for this result is that the nitric acid treatment leaves a Cr-rich iron oxide layer, which is more resistant to attack by I_2 and more resistant to FeI_xO_y film growth. The relative stability of the Cr-rich oxides slows the adsorption process and limits the adsorption to small defect locations. The effect of surface treatments will be examined more thoroughly in subsequent publications. The intention of this work was to understand the general processes involved in the interaction of iodine with stainless steel. It was felt that the untreated surface provided the most general example of this interaction.

5. Conclusions

The study has shown that iodine is initially adsorbed on stainless steel as metal iodides, probably as FeI_2, formed by the reaction with Fe in an oxidation state less than +2. The total amount of Fe used by iodine reaction and by further corrosion by oxygen on untreated stainless steel surfaces was extensive at room temperature, particularly in air. The adsorbed iodine desorbed only during purging with air, and not completely. The fraction of iodine which became fixed to the surface became larger with successive cycles, although the desorption that did occur appeared to follow similar first-order rates. This desorption behaviour and the extensive iodine-catalysed corrosion in air are explained by the reaction of oxygen with FeI_2 to form iron oxy-iodide (FeI_xO_y) scale. It is in the FeI_xO_y scale that the non-desorbing fraction of the iodine appears to be held. Significant volume changes that are due to the formation of FeI_2 and FeI_xO_y scale could continuously generate cracks through which I_2 can diffuse for further reaction with Fe.

The chemistry is clearly complex and there is a very strong interaction between competing reactions to form iron iodides, iron oxides and iron oxy-iodides. Although the mechanisms for the reactions are not yet fully understood, it appears that the physical and chemical properties of the corrosion scale strongly influence the rate of iodine uptake, the adsorption limit, and availability of iodine for later release. All these factors play a role in the prediction of iodine behaviour under the changing conditions that may be experienced following a reactor accident.

In conclusion, the reaction of stainless steel with I_2 is a relatively rapid process, even under mild conditions. The key reactions have been identified from which a semi-mechanistic kinetic model for the iodine interaction with stainless steel under certain conditions can be developed. However, the results obtained so far are insufficient either to support firm conclusions on the rate controlling processes, or to derive all the parameters required to fully model iodine behaviour with stainless steel under all conditions. The kinetic model development work is presented in a separate document [43].

Acknowledgements

The authors would like to thank Drs D.J. Wren, D.W. Shoesmith, P. Taylor and I.J. Muir at AECL and Mr K. Weaver at Ontario Hydro for helpful discussion and editorial comments. This work was funded by the CANDU Owners Group under the joint participation of Ontario Hydro, Hydro Quebec, New Brunswick Power and AECL.

References

[1] F. Garisto, Thermodynamics of iodine, cesium and tellurium in the primary heat transport system under accident conditions, Atomic Energy of Canada Limited Report, AECL-7782 (1982).
[2] D.J. Wren, Kinetics of iodine and cesium reactions in the CANDU reactor primary heat transport system under accident conditions, Atomic Energy of Canada Limited Report, AECL-7781 (1983).
[3] D. Cubicciotti, J.E. Sanecki, J. Nucl. Mater. 78 (1978) 96.
[4] C.V. McIsaac, D.G. Keefer, ACS Symp. Ser. 293 (1986) 168.
[5] J.J. DiNunno, Calculation of distance factors for power and test reactor sites, Technical Information Documents, TID-14844, US Atomic Energy Commission, 1962.
[6] L. Soffer, S.B. Burson, C.M. Ferrell, R.Y. Lee, J.N. Ridgely, Accident source terms for light-water nuclear power plants, USNRC Report, NUREG-1465, February, 1995.
[7] F. Funke, S. Hellmann, Reaction of iodine with steel surfaces – final report part 1: Literature study European commission, Nuclear Science and Technology, EUR 15668/1 EN, 1994.
[8] E. Hoinkis, A Review of the Adsorption of Iodine on Metal and its Behaviour in Loops, ORNL-TM-2916, 1970.
[9] T. Funuda, S. Omori, Corrosion of AISI 316 and AISI 304 Stainless Steel with Iodine Vapour, ORNL-TR-4694, 1975.
[10] R.M. Watkins, Corrosion of Stainless Steel by Iodine Vapour in the HTGR Fission Product Purge System, GAMD-1330, 1960.
[11] J. Abrefah, H.F.G. De Abreu, F. Tehranian, Y.S. Kim, D.R. Olander, Nucl. Technol. 105 (1994) 137.
[12] H.S. Rosenberg, J.M. Genco, D.L. Morrison, Fission Product Retention and Its Enhancement under Reactor Accident Conditions: Deposition on Containment-System Surfaces, BMI-1865, 1969.
[13] J.M. Genco, W.E. Berry, H.S. Rosenberg, D.L. Morrison, Fission-Product Deposition and Its Enhancement under

Reactor Accident Conditions: Deposition on Primary-system Surfaces, BMI-1863, 1969.
[14] J.M. Genco, H.S. Rosenberg, D.L. Morrison, Nucl. Safety 9 (1968) 226.
[15] J.B. Morris, B. Nichols, The Deposition of Iodine on Metal Surfaces, AERE-R 4502, 1965.
[16] C.E. Milstead, W.E. Bell, J.H. Norman, Nucl. Appl. 7 (1969) 361.
[17] G. Nishio, S. Kitani, Y. Ito, J. Nucl. Sci. Technol. 11 (1974) 339.
[18] M.F. Osborne, R.B. Briggs, R.P. Wichner, Iodine Sorption on Low-Chromium Alloy Steel, ORNL/TM-7755, 1982.
[19] M.F. Osborne, E.L. Compere, H.J. de Nordwall, Studies of Iodine Adsorption and Desorption on HTGR Coolant Circuit Materials, ORNL/TM-5094, 1976.
[20] M.F. Osborne, R.B. Briggs, Trans. Am. Nucl. Soc. 33 (1979) 294.
[21] M.F. Osborne, R.B. Briggs, R.P. Wichner, Sorption of Iodine on Low-Chromium Alloy Steel, Meeting of the American Nuclear Society, Fl, June 7–12, 1981.
[22] M.F. Osborne, R.B. Briggs, American Nuclear Society, Winter Meeting, San Francisco, November 11–16, 1979.
[23] F.H. Neil, Adsorption and Desorption of Iodine on Mild Steel, ORNL-TM-2763, 1970.
[24] E. Hoinkis, "Surface Interactions of Iodine with Fe_3O_4", Conf. and Exb. on Surface Studies, Guildford, Surrey, 10 July 1972.
[25] E. Hoinkis, Vacuum 22 (11) (1972) 525.
[26] A.W. Barsell, O.P. Chawla, C.G. Hoot, Safety Research on Iodine Plateout During Postulated HTGR Core Heat-up Events, Spec. Meet, on Coolant Chem., Plate-out and Contamination in Gas-Cooled Reactors, Julich, Germany, 2–4 December, 1980.
[27] J.A. Beavers, W.E. Berry, J.C. Griess, Proc. Int. Congr. Met. Corros. 3 (1984) 274.
[28] A.M. Beard, B.R. Bowsher, A.L. Nichols, Proc. Severe. Accident In Nuclear Power Plants, Sorrento 2 (1988) 201.
[29] R.D. Burnett, D.R. Lofing, C.C. Allen, Sorption of Iodine on Metal Surfaces (Dynamic Method), GA-8270, 1967, p. 143.
[30] S.L. Nicolosi, P. Baybutt, Vapour Deposition Velocity Measurements and Correlations for Iodine and Cesium Iodide, BMI-2091, 1982.
[31] D.L. Gray, F.H. Neill, Fission Product Transport and Deposition, ORNL-4200, 1967.
[32] S.A. Mucklejohn, N.W. O'Brien, T.R. Brumleve, J. Phys. Chem. 89 (1975) 2409.
[33] G.J. Evans, C. Deir, J.M. Ball, The retention of iodine on stainless steel sample lines, in: Proceedings of the 23rd DOE/NRC Nuclear Air Cleaning Conference. NUREG/CP-0141, Conf-940738, 1995, p. 279.
[34] C.A. Deir, A Study of the Interactions of Gas Phase Molecular Iodine With Stainless Steel Tubing, Math. Appl. Sci. Thesis, University of Toronto, 1995.
[35] J.W. Tyler, J. Nucl. Materials 161 (1989) 72.
[36] D.R. Lide, CRC Handbook of Physics and Chemistry 71st Ed., CRC, Boston, 1991.
[37] R.W.G. Wyckoff, Crystal Structures, 2nd ed., Vol. 1, Interscience, New York, 1963, p. 268.
[38] T. Tsukaue, G. Nakao, Y. Takimoto, K. Yoshida, Corros. Sci. 50, 755.
[39] M.G. Fontana, High Temperature Corrosion, in: Corrosion Engineer, 3rd ed., McGraw-Hill, New York.
[40] J.C. Wren, J.M. Ball, G.A. Glowa, R. Portman, G.G. Sanipelli, The interaction of iodine with organic material in containment, in: Proceedings of the Fourth CSNI/OECD Workshop on the Chemistry of Iodine in Reactor Safety, Wurenlingen, Switzerland, 1996.
[41] J.C. Wren, G.A. Glowa, J.M. Ball, Modelling iodine behaviour using Liric 3.0, in: Proceedings of the Fourth CSNI/OECD Workshop on the Chemistry of Iodine in Reactor Safety, Wurenlingen, Switzerland, 1996.
[42] J.M. Ball, W.C.H. Kupferschmidt, J.C. Wren, Results from phase 2 of the radioiodine test facility experimental program in: Proceedings of the Fourth CSNI/OECD Workshop on the Chemistry of Iodine in Reactor Safety, Wurenlingen, Switzerland, 1996.
[43] J.C. Wren, G.A. Glowa, J. Merritt, Modeling gaseous iodine adsorption onto stainless steel, J. Nucl. Materials, 1998, submitted.